Inductive transition of niobium and tantalum in the 10-MHz range. I. Zero-field superconducting penetration depth*

C. Varmazis†
Columbia University, New York, New York 10027
and Brookhaven National Laboratory, Upton, New York 11973

Myron Strongin
Brookhaven National Laboratory, Upton, New York 11973
(Received 29 April 1974)

The inductive transition of superconducting Nb and Ta was investigated at 15 MHz. These measurements provide values of $\lambda_L(0)$ for both Nb and Ta which are compared with other work. Particular attention has been given to impurities at the metal surfaces, and to how λ is affected through a change in the boundary condition on the Ginzburg-Landau order parameter. We emphasize that in accurate measurements the surface must be characterized by a parameter describing the slope of the order parameter at the surface. A peak in the inductive skin depth has been observed in the region very close to T_c, where $\lambda > \delta$, and this allows T_c to be determined very precisely.

I. INTRODUCTION

In this series of papers we present detailed measurements of the rf inductive transition of two transition-metal superconductors. This is an old problem, and the present measurements and analyses extend older results in two important ways. First, attention has been given to surface impurities, their removal, and their effect on the measurements. The effect of a nonideal surface is to make the slope of the Ginzburg-Landau order parameter nonzero, which increases the field penetration in the superconducting state. The parameter which describes this effect is the ratio $\xi(0)/b$, where $1/b = (1/\psi)(d\psi/dx)$. This parameter has already been used by Hopkins and Finnemore[1] in describing experiments on surface superconductivity in niobium, and we emphasize that in materials where surface impurities are important, this parameter characterizes the surface of the material.

Second, in previous measurements of the penetration depth, T_c was considered to be a parameter that was not accurately determined within the width of the transition. In the present measurements we have observed a peak in the inductive skin depth which allows an independent criterion for T_c, which we will discuss. This allows fits to the data to within millidegrees of T_c in pure Nb. The details of this phenomenon will be discussed in a second paper.[2]

It is interesting to point out that in obtaining $\lambda(0)$, one plots the penetration-depth data vs $Z(T)$ and then obtains $d\lambda(T)/dZ(T) = \lambda(0)$. Hence $\lambda(0)$ is not measured absolutely, and is only obtained from the temperature dependence of the inductance or some similar quantity. This makes the distinction between different theories extremely difficult.

In this first paper we discuss the zero-field penetration depth, the effect of different surface conditions, and the analysis of the data close to T_c. In a second paper we will discuss the peak in the inductive skin depth in some detail, as mentioned previously, and in a third paper we will discuss the transition in a small magnetic field, where interesting results are obtained due to fluctuations in the conductivity above T_c.

II. EXPERIMENTAL

The apparatus for the present measurements is shown in Fig. 1. The sample was contained in a superconducting coil which was part of the LC section of a tunnel-diode oscillator. The circuit elements were epoxied to a sapphire block which was cooled by conduction to the copper block extending from the O-ring flange. The vacuum can was attached to the O-ring flange by means of an indium O-ring, and was immersed in liquid helium during the runs. The sample was not touching the coil, and its temperature was varied with the heater shown in Fig. 1. With a superconducting coil and all the components at a constant temperature near 4.2 °K, stabilities of one part in 10^7 were routinely attained.

The tunnel-diode-oscillator circuit arrangement is shown in Fig. 2. This type of circuit is standard by now[3] and discussion is unnecessary except to emphasize again that the critical oscillator components were in the cryostat, which minimized problems of stray inductances and allowed operation at frequencies in the megacycle range. High-frequency operation is important if one wants to achieve a small enough normal-state skin depth, so that the condiction where $\lambda(T) > \delta$ can be achieved in an accessible temperature range. The

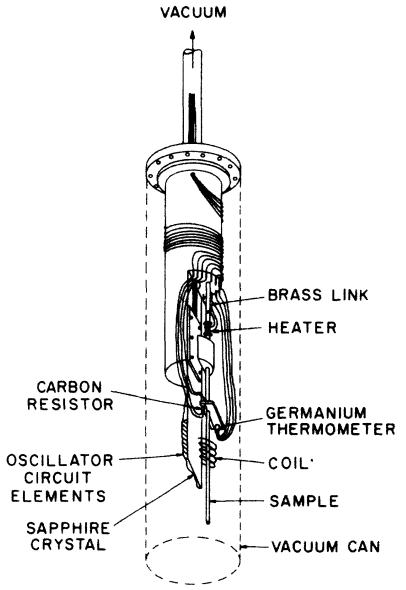

FIG. 1. General plan of low-temperature part of the tunnel-diode oscillator apparatus.

inductance changes due to the penetration-depth changes were determined by a frequency measurement and then displayed on an x-y recorder by means of a digital-to-analog converter.

A. Principle of measurement and calibration

The inductance of the solenoid containing the sample is proportional to the cross-sectional area of the space occupied by the flux. This includes the space between the coil and the sample, plus whatever distance the flux penetrates into the sample. As the temperature was changed below T_c the penetration depth changed, and thus the inductance changed. To calibrate the apparatus to attain λ values from the frequency changes with temperature, we follow the analysis given by Schawlow and Devlin. The basis of the analysis is the expression

$$\Delta L/L = \Delta\lambda 2\pi R/A \ , \tag{1}$$

where ΔL is the inductance change due to changes in λ given by $\Delta\lambda$, and A is the total area containing the flux, given by $A = \pi R'^2 - \pi R^2$, where R' is the effective coil radius and R is the radius of the region of flux exclusion in the sample. Then since

$$\omega^2 = 1/LC \ ,$$

$$\frac{\delta\omega}{\omega} = \frac{\delta f}{f} = -\frac{1}{2}\left(\frac{\delta L}{L}\right) = -\frac{1}{2}\left(\frac{2\pi R\delta\lambda}{A}\right) \ ,$$

and

$$\delta\lambda = -\left(\frac{\delta f}{f}\right)\frac{A}{\pi R} \ . \tag{2}$$

To remove the area dependence, one can now write that A, which is proportional to the inductance, must go as $1/f^2$, and one can then write that

$$A = D/f^2$$

and

$$\frac{d\lambda}{df} = -\frac{1}{f^3}\frac{D}{\pi R} \ . \tag{3}$$

To make the correspondence with the notation of Schawlow and Devlin[4] one can write

$$d\lambda = dR$$

and therefore

$$R\,dR = -\frac{df}{f^3}\frac{D}{\pi} \ ,$$

$$R^2 = +(1/f^2)(D/\pi) + K \ ,$$

or

$$\frac{1}{f^2} = \frac{\pi}{D}R^2 - \frac{K\pi}{D} = BR^2 + C \ ,$$

and finally in the form of Ref. 4,

$$\frac{d\lambda}{df} = \frac{-1}{f^3}\frac{1}{BR} \ . \tag{4}$$

Hence by using specimens of different diameter and measuring f, one can obtain B and an expression for $d\lambda/df$. Assuming that the penetration depth is a function of the form $\lambda(T) = \lambda(0)Z(T)$, we have $d\lambda/dZ = \lambda(0)$. $Z(T)$ is a theoretical temperature dependence given by the BCS theory or the phenomenological theory. Then to find $\lambda(0)$ we have

$$\frac{d\lambda}{dZ} = -\frac{1}{BR}\frac{1}{f^3}\frac{df}{dZ} \ . \tag{5}$$

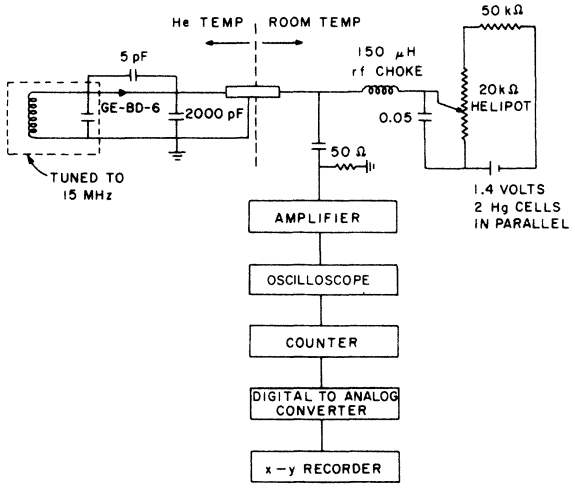

FIG. 2. Tunnel-diode oscillator circuit.

The actual measurements give the variation of f vs T. From that variation f vs $Z(T)$ is obtained, and finally the slope df/dZ. The absolute value of $\lambda(0)$ is then obtained from a knowledge of the sample radius and B.

In the above analysis it is assumed that $\Delta f/f = -\Delta L/2L$, which is strictly true in the limit of infinite circuit Q. A more exact expression is that $\Delta f/f = -(\Delta L/2L)(1-2/Q^2) - \Delta R/RQ^2$. From an analysis of the circuit elements, we estimate that $Q > 1000$, and hence $\Delta f/f = -\Delta L/2L$ is an excellent approximation. This is consistent with other estimates of Q for an LC circuit using a superconducting coil. It should be mentioned that stable oscillations can, in fact, only be attained with a BD-6 diode when $Q \gtrsim 250$. Hence as long as the diode oscillates, the resistive changes are down many orders of magnitude from the inductive changes.

III. THEORY—GENERAL

In this paper we do not intend to give a detailed description of the BCS theory of the penetration depth, since this has been done by many others. Instead we concentrate on aspects of the theory which have not been treated carefully, such as the effect of surface-boundary conditions and an analysis of the inductive skin depth and its relationship to λ. Before considering these problems, we mention briefly that we have analyzed the data for high Z, using the local BCS function for Z as tabulated by Muhlschlegel.[5] In this case the expression for $\lambda_L(T)$, the London penetration depth becomes $\lambda_L(T) = Z_{\rm BCS}(T)\lambda_L(0)$, where $\lambda_L^{-2}(0) = 4\pi n_s e^2/mc^2$. Near T_c, the ratio of the observed or BCS value of the penetration depth $\lambda(T)$ to $\lambda_L(T)$ becomes unity, and therefore near T_c

$$\frac{d\lambda(T)}{dZ_{\rm BCS}} = \frac{d\lambda_L(T)}{dZ} = \lambda_L(0) \ . \tag{6}$$

It should be mentioned that much data have been analyzed on the basis of the Gorter-Casimir phenomenological theory, where

$$Z_{\rm GC}(T) = (1-t^4)^{-1/2} \ .$$

Near T_c,

$$\lambda_{\rm BCS}(T) = \lambda_L(0)/\sqrt{2}\,(1-t)^{1/2} = \lambda_L(0) Z_{\rm BCS} \tag{7}$$

and

$$\lambda_{\rm GC} = \lambda_{\rm GC}(0)/2(1-t)^{1/2} = \lambda_{\rm GC}(0) Z_{\rm BCS}/\sqrt{2} \ , \tag{8}$$

giving $\lambda_{\rm GC}(0) = \lambda_L(0)\sqrt{2}$, since near T_c the observed penetration depth $\lambda(T) = \lambda_{\rm BCS}(T) = \lambda_{\rm GC}(T)$. Finally, it is clear that near T_c

$$\sqrt{2}\,\frac{d\lambda(T)}{dZ_{\rm BCS}} = \frac{d\lambda(T)}{dZ_{\rm GC}} \ . \tag{9}$$

If not specified, we have generally used $\lambda(T)$ to be the observed penetration depth, which is assumed to be the $\lambda_{\rm BCS}$ on the assumption that this theory is correct.

A. Analysis of inductive skin depth and the relationship to λ

In this section we briefly discuss the definition of the inductive skin depth, which is the property of the sample which determines the coil inductance in the limit of high Q. We can write the equation for field penetration as

$$h = h_0 e^{i\omega t - iKZ} \ ,$$

where from the London theory[6]

$$-K^2 = (1/\lambda^2 + 2i/\delta^2) \tag{10}$$

and the definition of δ is $1/\delta^2 = 2\pi\omega\sigma/C^2$). Below T_c, δ is the skin depth of the normal electrons, and above T_c it is the usual skin depth.

This can be cast in terms of the real and imaginary parts of the surface impedance where

$$R_s = (4\pi\omega/c^2)[{\rm Re}(1/K)] \tag{11}$$

and

$$X_s = (4\pi\omega/c^2)[{\rm Im}(1/K)] \ . \tag{12}$$

By definition

$$\delta_r = (c^2/4\pi\omega) R_s \tag{13}$$

and

$$\delta_i = (c^2/4\pi\omega) X_s \ . \tag{14}$$

From Eq. 10 we have

$$1/K = i(1/\lambda^2 + 2i/\delta^2)^{-1/2} \ , \tag{15}$$

$${\rm Im}(1/K) = (1/\lambda^4 + 4/\delta^4)^{-1/4} \cos\tfrac{1}{2}[\tan^{-1}(2\lambda^2/\delta^2)] = \delta_i \ . \tag{16}$$

Note that when $\delta \gg \lambda$, which is the condition during most of the measurements to be discussed, then $\delta_i = \lambda$; and in the normal state, when $\lambda = \infty$, then $\delta_i = \frac{1}{2}\delta$.

In the region very close to and below T_c, where $\lambda > \delta$, we will show in Ref. 2 that

$$\frac{d\delta_i}{dT} = \frac{1}{4}\left(\frac{-\delta^3}{\lambda^3}\right)\frac{d\lambda}{dT} \ . \tag{17}$$

Hence, as T goes below T_c, λ gets smaller; and since $d\delta_i/dT$ is negative, it means δ_i increases as T gets smaller. Finally, when $\lambda \ll \delta$, δ_i goes to λ and hence there must be a peak in δ_i close to T_c. This peak is illustrated in the transitions shown in Figs. 3 and 4.

B. Effect of surface boundary conditions on λ

The usual analysis of the penetration depth involves the solution of the London equations with the usual definition that $\lambda_L^2 = c^2/16\pi\psi_0^2 e^2$. With the BCS theory, the equations are appropriately modified

to take into account, more realistically, the details of the electrodynamics. However, in the context of the Ginzburg-Landau theory, most analyses assume essentially constant order parameter in the sample with the boundary condition that $d\psi/dx = 0$. Clearly if $d\psi/dx \neq 0$, i.e., suppose, for example, there is a normal layer on the surface, λ will change and will in fact be increased, if the order parameter is somewhat smaller in the surface regime. This problem has been treated by de Gennes and Matricon,[7] and we briefly summarize their analysis below. In addition, we have numerical values for λ_{eff}/λ in the general zero-field case which are useful in analyzing actual data. Note that in this analysis it is assumed that there is no shielding due to the normal layer.

We consider the one-dimensional Ginzburg-Landau equation for the half-plane $x > 0$, with the field H_z in the Z direction. Then the Ginzburg-Landau equation in zero field is

$$-\xi^2(T)\frac{d^2f}{dx^2} - f + f^3 = 0 , \tag{18}$$

where

$$f = \psi/\psi_0 .$$

This can be cast in the form

$$\xi^2(T)\left(\frac{df}{dx}\right)^2 = \tfrac{1}{2}(1-f^2)^2 \tag{19}$$

with a solution

$$f = \tanh\left[(x - x_0)/\sqrt{2}\,\xi(T)\right] . \tag{20}$$

x_0 is determined from the boundary condition that

$$\left(\frac{1}{f}\right)\frac{df}{dx}\bigg|_{x=0} = \frac{1}{b} . \tag{21}$$

In the case of the metal-vacuum interface, $b \to \infty$, whereas in the case of a thick normal layer on the surface, b approaches the coherence length in the normal metal.

By differentiating Eq. (20), one finds the relationship for x_0 in terms of b given below:

$$1 - \tanh^2\frac{x_0}{\sqrt{2}\,\xi(T)} = -\sqrt{2}\left(\frac{\xi(T)}{b}\right)\tanh\frac{x_0}{\sqrt{2}\,\xi(T)} .$$

If we now consider the case of a weak magnetic field in the Z direction, then we have the additional equation

$$\frac{\partial^2 A_y(x)}{\partial x^2} = \frac{16\pi e^2}{mc^2}\,|\psi_0|^2 f^2 A_y ,$$

which takes the form

$$\frac{\partial^2 A_y}{\partial x^2} = \frac{f^2}{\lambda(T)^2}A_y , \tag{22}$$

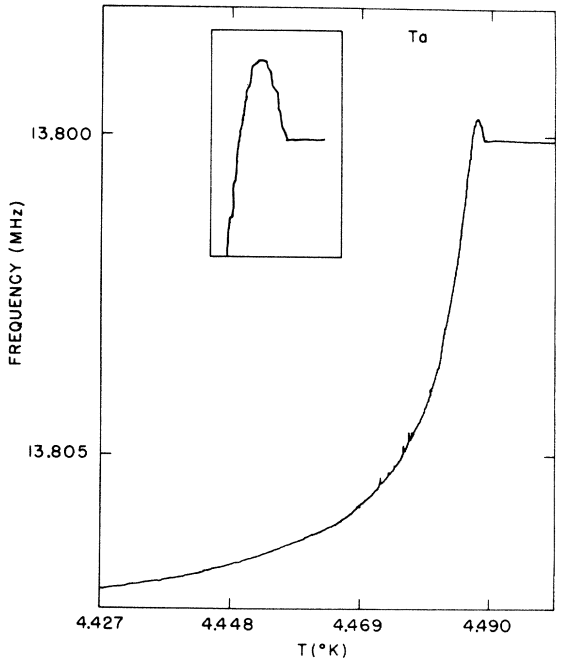

FIG. 3. Transition for relatively clean Ta sample with resistance ratio of 600. Note that the inset shows the δ_i peak, and that there is very little curvature above T_c.

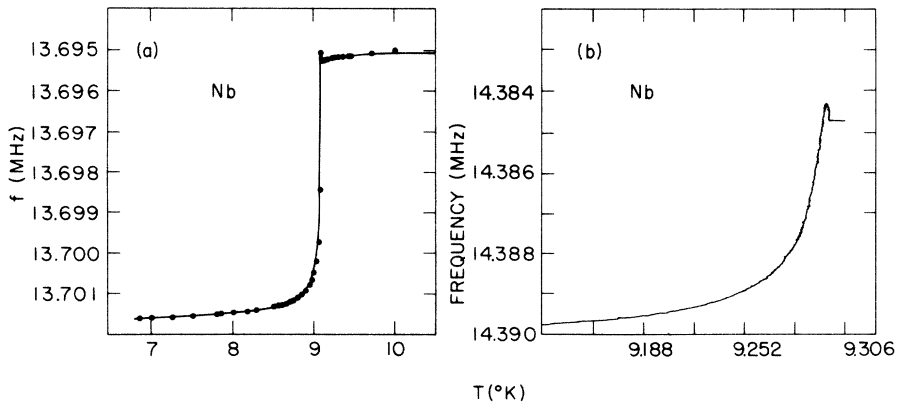

FIG. 4. (a) Nb transition with RRR > 750, showing curvature above T_c. (b) Nb transition with RRR > 750 shows peak in δ_i, but little curvature above T_c.

where we can take the weak-field value for f given by Eq. (20). If we now let

$$\theta = (x - x_0)/\sqrt{2}\,\xi(T)$$

we have $f = \tanh\theta$ and

$$\frac{\partial^2 A_y}{\partial\theta^2} = \left(\frac{2f^2\xi^2(T)}{\lambda^2(T)}\right)A_y = \frac{2f^2}{\kappa^2}A_y ,$$

and finally

$$\frac{\partial^2 A_y}{\partial\theta^2} + \left(-\frac{2}{\kappa^2} + \frac{2/\kappa^2}{\cosh^2\theta}\right)A_y = 0 . \tag{23}$$

The solution of this equation is given in Landau and Lifshitz[8]; defining

$$\lambda_{eff} = \frac{A_y}{H}\bigg|_{x=0} = \frac{A_y}{\partial A_y/\partial x}\bigg|_{x=0} ,$$

and have

$$\frac{\lambda_{eff}}{\lambda} = \frac{\sqrt{2}}{\kappa}\,\frac{F}{(1/m)\tanh\theta_0 F + (ij/2k)[F'(1-\tanh^2\theta_0)]} , \tag{24}$$

where

$$F = F[i;\, j;\, k;\, \tfrac{1}{2}(1-\tanh\theta_0)]$$

and

$$F' = F'[i+1;\, j+1;\, k+1;\, \tfrac{1}{2}(1-\tanh\theta_0)]$$

are hypergeometric functions with

$$i = 1/m - s , \quad j = 1/m + s + 1, \quad k = 1/m + 1 ,$$

and

$$2/\kappa^2 = s(s+1) = 1/m^2 .$$

When

$$b/\xi(T) \to 0$$

we have $\tanh\theta_0 = 0$, and the above expression reduces to

$$\frac{\lambda_{eff}}{\lambda} = \frac{1}{\sqrt{2}\,\kappa}\,\frac{\Gamma(-\frac{1}{2}s + 1/\kappa\sqrt{2})\Gamma(\frac{1}{2} + \frac{1}{2}s + 1/\kappa\sqrt{2})}{\Gamma(\frac{1}{2} - \frac{1}{2}s + 1/\kappa\sqrt{2})\Gamma(1 + \frac{1}{2}s + 1/\kappa\sqrt{2})} , \tag{25}$$

which is the expression given by de Gennes and Matricon.[7] In the Table I, we have included tables of computer plots of the general case of λ_{eff}/λ as a function of ξ/b for $\kappa = 0.4$ and 0.8, which correspond essentially to the κ's for Nb and Ta. Actually, in the limit of $\xi/b \to \infty$, de Gennes and Matricon have obtained the results that when

$$\kappa \to 0 , \quad \frac{\lambda_{eff}}{\lambda} = 1.76\kappa^{-1/2} ,$$

when

$$\kappa = 1/\sqrt{2} , \quad \frac{\lambda_{eff}}{\lambda} \sim 2.3 ,$$

and when

$$\kappa \gg 1 , \quad \frac{\lambda_{eff}}{\lambda} = 1 .$$

TABLE I. Variation of λ_{eff}/λ with $\xi(T)/b$ for two κ values.

$\kappa = 0.4$		$\kappa = 0.8$	
$\xi(T)/b$	λ_{eff}/λ	$\xi(T)/b$	λ_{eff}/λ
0.01	1.006	0.01	1.005
0.02	1.011	0.02	1.009
0.03	1.017	0.03	1.014
0.04	1.022	0.04	1.018
0.05	1.028	0.05	1.023
0.06	1.033	0.06	1.027
0.07	1.039	0.07	1.032
0.08	1.045	0.08	1.036
0.09	1.050	0.09	1.041
0.1	1.056	0.1	1.045
0.12	1.067	0.12	1.054
0.16	1.090	0.16	1.072
0.2	1.113	0.2	1.090
0.25	1.142	0.25	1.113
0.3	1.171	0.3	1.135
0.4	1.229	0.4	1.179
0.6	1.344	0.6	1.264
0.8	1.454	0.8	1.342
1	1.559	1	1.413
2.01	1.966	2.01	1.667
3.01	2.21	3.01	1.806
4.01	2.362	4.01	1.880
5.01	2.464	5.01	1.943
6.01	2.536	6.01	1.981
7.01	2.59	7.01	2.009
8.01	2.631	8.01	2.03
9.01	2.664	9.01	2.046
9.96	2.689	9.96	2.059

From computer computations from Eq. (25), for $\kappa = 0.2$, we can take the value for $\xi/b = 10$, which gives $\lambda_{eff}/\lambda = 3.55$. From the expression $\lambda_{eff}/\lambda = 1.76\kappa^{-1/2}$, we get $\lambda_{eff}/\lambda \sim 3.93$, in approximate agreement with the above estimate. For $\kappa = 0.707$, computations give $\lambda_{eff}/\lambda \sim 2.16$ for $\xi/b \sim 10$, which is in reasonable agreement with 2.3. It is certainly clear that for κ's of the order of 1, as in Nb and Ta, the ratio of λ_{eff}/λ deviates significantly from unity as one approaches T_c, and it will be seen that this can have a significant effect on the data.

IV. SAMPLE PREPARATION

The preparation of clean niobium and tantalum surfaces is a complex and essentially impossible task if the samples are removed from an ultrahigh vacuum environment. Studies at Brookhaven have shown that oxygen in the bulk of the sample migrates to the surface of both Nb and Ta upon cooling from high-temperature anneals,[9,10] and recent work by Joshi and Strongin[10] has established that the oxygen distribution returns to the bulk distribution in the order of a few monolayers. We do not intend to discuss these questions in detail here, but it is important to mention that even the most carefully prepared samples of these metals will

TABLE II. Steady-state oxygen concentrations at various pressures. For discussion see Ref. 9.

	log$C$		
T(°K)	$P = 10^{-6}$ Torr	$P = 10^{-8}$ Torr	$P = 10^{-9}$ Torr
1873	−0.43	−2.43	−3.43
1973	−0.89	−2.89	−3.89
2073	−1.29	−3.29	−4.29
2173	−1.66	−3.66	−4.66
2273	−2	−4	−5

not have perfect surfaces. It will be shown that heating niobium in oxygen leads to an apparent large value of λ which we now think is mainly due to faceting[11] of the surface and increased roughness, a factor which will be discussed later.

To prepare our cleanest samples, MRC Marz-grade niobium wire was electropolished with a mixture of HF and H_2SO_4 at 0 °C. The samples were then heated to 1800 °C in 10^{-7} Torr of oxygen to remove carbon and promote grain growth[12]; Then the samples were heated at pressures less than 10^{-8} Torr, and temperatures over 2000 °C for Nb, and about 2500 °C for Ta. Electron and optical microscopy indicated relatively smooth surfaces and only a few large grains in the region enclosed by the measuring coil.

To study the effects of heating in oxygen, the samples were heated at temperatures near 1800 °C in the 10^{-6} Torr range to achieve different bulk oxygen concentrations. In Table II, some steady-state oxygen concentrations are given for different temperatures and pressures. The amount of oxygen in the bulk was estimated from the resistance ratio and from the result from Pasternak and Evans[13] that $\Delta\rho/\rho \sim 0.3$ at.%. The changes in T_c were consistent in that T_c dropped at about the rate given by de Sorbo,[14] of 1 °K/at.%.

V. DATA

A. Normal state

The normal-state properties of the bulk were determined from the resistance ratio between 10 and 300 °K. The resistance ratios ranged about 80–1500, depending on the ambient pressure and temperature during the heating cycles. The steady-state oxygen concentrations in niobium are known for various temperatures and pressures, and by this technique varying amounts of oxygen could be put into the samples. However, thermal faceting occurred when the samples were heated near 1800 °C in pressures near 10^{-6} Torr,[11] and the increased perimeter due to the surface roughness made λ appear larger in these cases. This effect will be discussed later.

The resistivity values obtained from the resistance ratio checked nicely with the estimates from the normal-state skin depth. In Fig. 5 the skin depth is plotted as a function of the resistance ratio. The leveling off of the skin depth at the larger resistance ratios indicates that the anomalous skin effect regime is being approached.

Finally, there is one other phenomenon that should be mentioned in the context of normal-state behavior. In Fig. 3 we show the Ta transition and, in particular, the inset shows the region above T_c. It can be seen that the normal-state skin depth is independent of temperature in ths regime. In Fig. 4(a) it can be seen that this is not the case for Nb, and small changes in the skin depth can be seen a few tenths of a degree above the sharp transition. This is hard to understand on the basis of oxides, since a lower T_c would be expected. This small effect is observed to some extent on all niobium samples, although it can almost vanish, as in Fig. 4(b), and we tentatively associate this effect with the possibility of small amounts of carbide or other niobium carbon compounds on the niobium surface, which would have a T_c above bulk niobium. If the regions were disconnected and small in volume, a relatively small shielding effect would be observed in an ac measurement, as in the actual data. We have taken steps to remove carbon in all samples by heating in oxygen and then heating in ultrahigh vacuum, as discussed previously. Auger- and

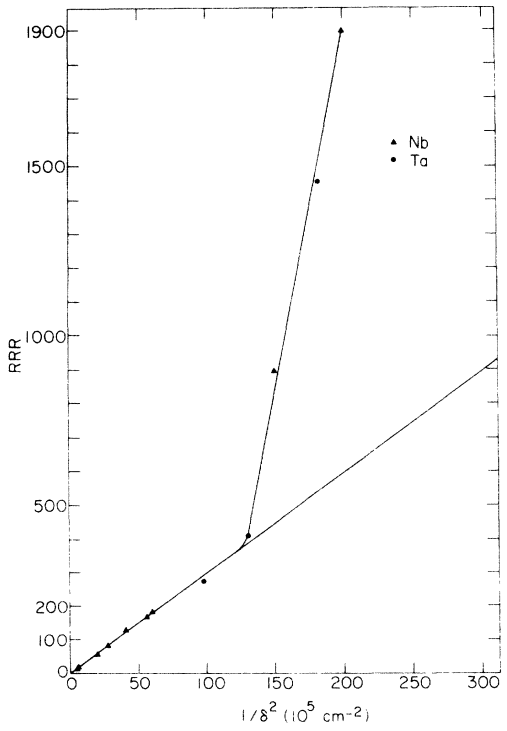

FIG. 5. Normal-state skin depth vs residual resistance ratio (RRR). The leveling off at large resistance ratio values is indicative of the anomalous regime.

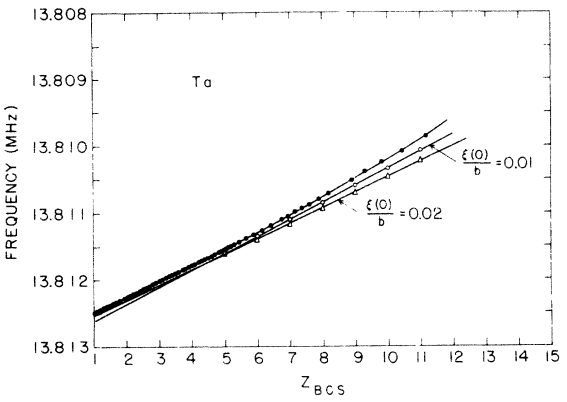

FIG. 6. f vs Z_{BCS} for clean Ta with RRR > 600. The curvature is removed for $\xi(0)/b \sim 0.02$.

mass-spectroscopy studies have confirmed that this procedure leads to carbon removal. However, a very small residual effect above T_c is observed even in our most carefully prepared samples, and this could mean carbides are still segregated on grain boundaries or other clusters, rather than being distributed uniformly along the surface. This particular feature of the niobium transition is not understood at this time, and further work remains to be done.

B. Clean Ta

The data for Ta are shown in Fig. 3, and the data plotted against the local BCS two-fluid function Z_{BCS} are shown in Fig. 6, in the region where $\lambda < \delta$. We emphasize that the value of T_c used in analyzing the data is not obtained by the usual procedure of getting a best fit to a linear function on the λ vs Z plot, but as mentioned previously, T_c is defined as the temperature at which the peak in δ_i starts. This, we feel, defines T_c to a few tenths of a millidegree and allows analysis of the data up to $Z \sim 15$, which is much closer to T_c than previous analyses, allowing data analysis in the local limit. However, any effects of boundary conditions are more severe in this region because $\xi(T)$ is also getting large near T_c. This point will be discussed more fully.

C. Nb

The data for clean Nb are shown in Fig. 4, and a characteristic plot of the oscillator frequency change vs $Z_{BCS}(T)$ is given in Fig. 7. In Fig. 8 we have the data for various oxygen concentrations plotted as a function of $Z(T)$. As the samples are heated in oxygen, two effects are evident: an increased curvature at high Z, and a change in the residual slope at low Z. As mentioned previously, these are real effects caused by imperfect surfaces, and will be discussed in the Sec. VI.

VI. DATA ANALYSIS—GENERAL COMMENTS

Because we have been able to obtain reliable data very close to T_c up to Z_{BCS} of about 20, we have emphasized this region in obtaining reliable values of $\lambda_L(0)$. We mention again that the peak in δ_i (shown, for example, in Fig. 3) allows T_c to be defined to less than one millidegree K. The advantage of data analysis in this regime is that for $l \gg \xi_0$, the ratio of $\lambda(T)/\lambda_L(T)$ is essentially unity for niobium, and differs from unity by less than 5% for Ta. Hence, with few assumptions and with rather small additional corrections, one can, in principle, get $\lambda_L(0)$ from Eq. (6). Because of the precision of the present data, we have been able to make even further refinements in the analysis to take account of normal surface layers, or of essentially anything that would affect the surface-boundary condition and the ratio of $\xi(T)/b$, whose effect is to give a ratio of $\lambda_{eff}(T)/\lambda(T) \sim \lambda_{eff}/\lambda_L(T)$ that deviates from unity as discussed previously. Because near T_c we can write $\xi(T) \sim Z(T)\xi(0)$ to a good approximation in the clean limit, it is clear that $\xi(T)/b$ gets larger near T_c and the ratio λ_{eff}/λ gets larger as shown in Table I. This leads to some small curvature, even in the clean sample data as shown in Figs. 6 and 7. Our method of analyzing the data has been to assume values of $\xi(0)/b$ as shown in Figs. 6 and 7, and to find $\lambda_{eff}(T)/\lambda(T)$ as a function of $\xi(0)Z/b$ near T_c. *The proper assumption for $\xi(0)/b$ yields a linear plot for high Z, and for small nonlocal corrections yields essentially $\lambda(T) \sim \lambda_L(T)$ vs Z, as shown.* The slope of this corrected curve $d\lambda_L(T)/dZ_{BCS}$ then gives $\lambda_L(0)$. Note that the intercept of the extrapolated curve at $Z = 1$ is $\lambda_L(0)$, and the ratio of the measured value to this value yields in principle the ratio $\lambda_{BCS}(0)/\lambda_L(0)$. In view of the corrections and the large extrapolation distance, we have not taken these values seriously enough to compare with theory, but rather as confirmation that our extrapolation to attain $\lambda_L(0)$ from the intercept is quite reasonable.

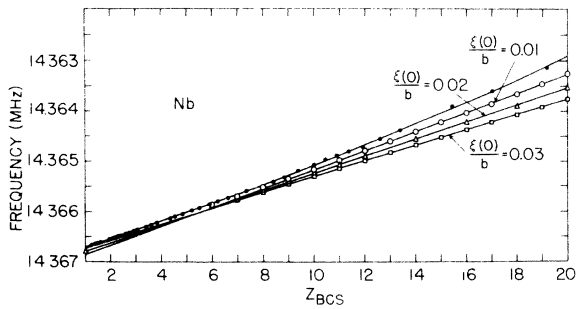

FIG. 7. f vs Z_{BCS} for clean Nb with RRR > 1000. Curvature is removed for $\xi(0)/b \sim 0.02$.

A. Ta data near T_c

Miller[15] has calculated the ratio $\lambda(T)/\lambda_L(T)$ near $T=0$, and near $T=T_c$, for various values of $\pi\xi_0/2l$, and taking these small corrections into account near T_c allows us to make a correction of a few percent on the procedure discussed in Sec. V. For clean Ta where the resistance ratio is >1000, $\pi\xi_0/2l < 0.05$, and $\lambda(T)/\lambda_L(T) \sim 1.04$ near $t=1$. Using the slope from Fig. 6 for the $\xi(0)/b=0.02$ corrected curve, we get $\lambda_L(0)=350\pm15$ Å. If we make the crude estimate that $b \sim \xi_N(\xi_N/d)$ for $0<d<\xi_N$, then a value of b of about $50\xi_N$ can be obtained with about 10 Å of normal material, i.e., $d\sim10$ Å. Note that near T_c, say for $Z=10$, $\xi(T)/b\sim0.2$, and from Table I, $\lambda_{eff}/\lambda\sim1.1$. Hence even a small number of normal layers can cause a rather large change in λ close to T_c. At $Z=1$, for example, $\xi(0)/b$ is 0.02, and the correction is of the order of 1%.

B. Niobium data near T_c

The clean-niobium data shown in Fig. 7 is similar in nature to the Ta data. Again, curvature in the measured values of λ vs Z are seen at high Z, and the curves have been corrected for different values of $\xi(0)/b$. The best fit was obtained for $\xi(0)/b$ of about 0.02, as shown in Fig. 7, which agrees well with measurements of Hopkins and Finnemore.[1] The nonlocal corrections are extremely small near T_c for Nb, and we have neglected them. The value obtained for $\lambda_L(0)$ was 315 Å, and from the extrapolation to 0 °K, or $Z=1$, we find a value of $\lambda_{BCS}(0)/\lambda L(0)$ of about 1.2, which is consistent with the value expected from the BCS theory. In Fig. 8 we show the data for niobium heated in oxygen, and the variety of effects that can occur. The curvature in the data is much greater than the clean case, and in fact the slope near $Z=1$ never approaches the value for clean niobium. We think two problems can be involved here. One is the geometrical effect caused by surface roughness and increased perimeter, and the other contribution to the curvature is caused by a larger value of $\xi(0)/b$ than the clean case. In Fig. 9 we show data for a Nb sample with residual resistance ratio (RRR) of 170 heated to over 1800 °C in an oxygen pressure of 8×10^{-7} Torr. It is interesting that although most of the curvature is removed by a value of $\xi(0)/b\sim0.20$, a linear dependence of $\lambda_L(T)$ vs $Z_{BCS}(T)$ is not obtained as in the clean case. The large value of the slope of $d\lambda/dZ$, even near $Z=1$, has been interpreted previously as an increased value of λ caused by a smaller mean free path (mfp) at the surface.[16] From Auger measurements of the falloff of oxygen in from the surface, which indicate a return to the bulk oxygen concentration

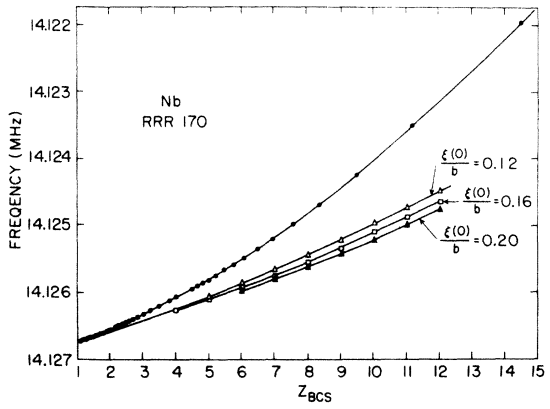

FIG. 9. f vs Z_{BCS} for Nb sample heated above 1800 °C at 8×10^{-7} Torr for 5 h. Curvature is never completely removed, even for $\xi(0)/b\sim0.2$.

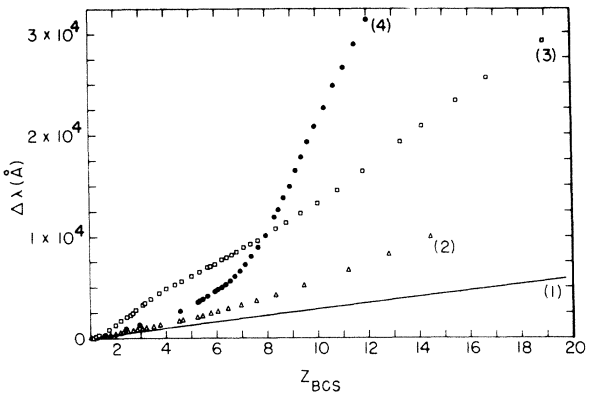

FIG. 8. Effect of oxygen on λ; curve (1)—clean Nb; curve (2)—RRR 170 heated at 8×10^{-7} Torr at ~1800 °C; curve (3)—RRR 85 heated over 1900 °C at 2×10^{-6} Torr; curve (4)—RRR 8 heated close to 1800 °C at 2×10^{-6} Torr.

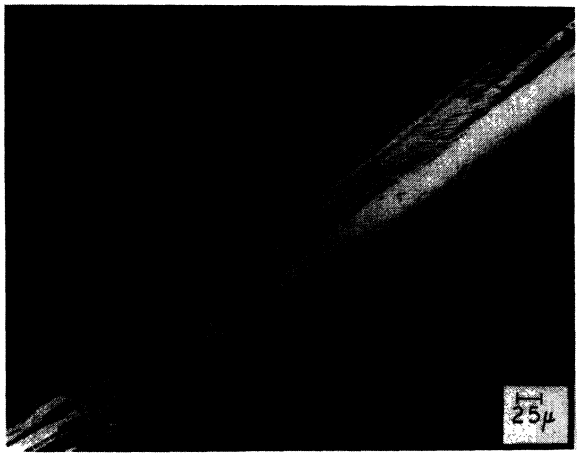

FIG. 10. Faceted surface, heated to over 1900 °C at 2×10^{-6} Torr for times of about 5 h.

in a few monolayers,[10] we do not think that the mfp at the surface can change by a factor of about 10 to explain increases of λ by up to a factor of 3. It appears more likely that heating in oxygen causes increased surface roughness[11] (see Fig. 10), due to thermal faceting, and in fact the perimeter of the sample is increased, which makes the area for current flow $2\pi R\lambda f$, where f is a geometrical factor which is greater than 1 for a rough surface, and equal to 1 for a smooth surface. The effect of surface roughness on measurements of λ has been previously discussed by Laurmann and Shoenberg.[17] Surface roughness can also cause an additional temperature dependence, since the diamagnetism of small protrusions will depend on the relative values of λ and the protrusion size. When $\lambda \ll a$, the radius of a characteristic protrusion, the usual temperature dependence will be attained. However, in the intermediate region where $\lambda \sim a$, an additional dependence will be obtained. Since the details of the surface roughness and the effects of normal layers cannot be separated, it is not profitable to pursue how λ is changed in these nonuniform samples.

C. Data near $Z = 1$

Most other investigators have analyzed their data in the regime where Z is of the order of about[4,18] 4 to 1, and it is probably worth discussing the present data in this regime. In analyzing the data it was assumed that the BCS theory was valid, and that a fit to the data near $Z = 10$, where the theory is local, gives $\lambda_L(0)$. Other investigators have fit the data to the Z values near 1, and have derived values for $\lambda_L(0)$ in this manner. Maxfield and McLean[18] have analyzed their data in the regime where $d\lambda/dZ_{GC}$ has curvature in it, i.e., for low Z_{GC}, and they find that a self-consistent analysis gives $\lambda_L(0) = 390$ Å, which implies deviations from the BCS theory. They find that the expression for the London parameter can be expanded in terms of $\beta\Delta(T)$ as $\Lambda/\Lambda_T = 0.213\beta^2\Delta(T)^2$, where $\beta = 1/kT$. Near T_c, $\Delta(T) = B(1-t)^{1/2}kT_c$ and

$$\lambda_L(0) = (0.213)^{1/2} B \frac{1}{2}\left(\frac{d\lambda}{dZ_{GC}}\right)_{T_c} . \qquad (26)$$

For Nb, near T_c, $d\lambda/dZ_{GC} = (\sqrt{2})(d\lambda/dZ_{BCS})$. If the BCS dependence holds, one can write $d\lambda/dZ_{BCS} = \lambda_L(0)$, which makes Eq. (26) an identity with $B = 3.1$, as expected from the BCS theory. Hence, in our analysis terms, we have assumed $B = 3.1$ since we have used the BCS expression that $(\sqrt{2})d\lambda/dZ_{BCS} = d\lambda/dZ_{GC}$. Actually we are not convinced that an analysis of the data near $Z = 1$ is reliable in the case of niobium or on material with a tendency to adsorb oxygen in the surface regime. In our data we observe very sharp bending in the f vs Z_{GC} plots in the region below $Z_{GC} < 1.2$ or $T \sim 6$ °K, as shown in Fig. 11. This bending is much sharper than can be expected from any theory describing a uniform sample, and we think that this rapid change of $d\lambda/dZ$ near $Z = 1$ is actually related to the normal monolayers discussed previously. It has been assumed that these monolayers give negligible shielding of the rf fields, which is probably a reasonable assumption when the layer is normal. However, when the layer becomes superconducting, there is additional shielding plus a small effect due to lifting the order parameter at the impure-Nb–pure-Nb interface, since b is now essentially ∞ at this interface. Both these effects make λ look smaller. The rapid drop is caused by the T_c being of the order of 6 °K, and by the fact that on this plot computed for the T_c of the bulk niobium, the impure layer goes from T_c to $T \ll T_c$ over the range of $Z = 1.2$ to $Z = 1$. The effect is consistent with about a 30-Å impure layer, which is in reasonable agreement with the estimates from the high Z values. The net result of these effects is to make data analysis very difficult in this region, and in the case of niobium, the situation is further complicated by a nonlocal correction of about 20% in this region. In fact, in the region above this rapid falloff, one can see that the ratio of the measured λ to λ_L is about 1.1 to 1.2, as one would expect from the BCS theory. At any rate, we feel that our data cannot be analyzed for deviations from the BCS theory, and we quote $\lambda_L(0)$ values assuming the constants as given by the BCS theory. For Ta, the low-temperature data show a similar falloff at low Z, although somewhat smaller in magnitude, and we suspect it involves similar considerations. Again, the $\lambda_L(0)$ values are attained from the fits near T_c adjusted by the nonlocal correction of 5%.

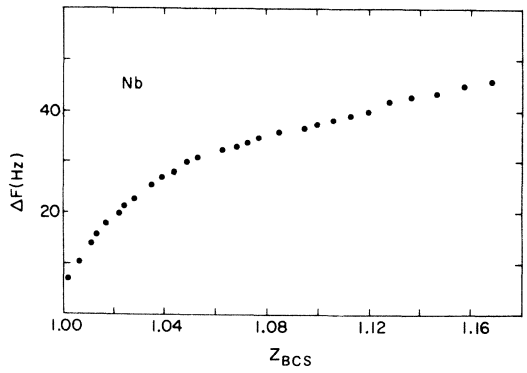

FIG. 11. Data near $Z = 1$, showing a sharp drop at the lowest temperatures.

D. Discussion of $\lambda_L(0)$ values

For Ta we find $\lambda_L(0) = 350 \pm 15$ Å. The Ginzburg-Landau (GL) parameter κ can be calculated

from the relationship of the GL theory

$$\kappa(T\sim T_c)=\frac{\lambda_L(0)^2\,2\pi\sqrt{2}H_c(0)}{\varphi_0}\quad . \tag{27}$$

Using $H_c(0)=820$ Oe, we attain $\kappa\sim 0.43$. The value of $\lambda_L(0)$ compares well with recent measurements, but our estimate of κ using $H_c(0)$ is somewhat higher than recent measurements, which give $\kappa\sim 0.36$.[19] These measurements start from essentially the same $\lambda_L(0)$ but use the formula for κ in terms of $dH_c(T)/dT$, and they attain $\kappa=0.36$. We do not understand the discrepancy which would imply a large deviation from a parabolic dependence for $H_c(T)$ assumed in the derivation of Eq. (27). ξ_0 can be calculated from the clean-limit relationship that $\kappa=0.96\ (\lambda_L(0)/\xi_0)$. Using $\kappa\sim 0.43$ and $\lambda_L(0)=350$ Å, we obtain $\xi_0=780$ Å.

For Nb, $\lambda_L(0)=315\pm 15$ Å, which checks well with the value given by Hopkins and Finnemore,[1] but this value is much lower than the value of 390 Å given by Maxfield and McClean.[18] We emphasize that we have assumed the validity of the BCS theory in the regime near T_c, and the data were analyzed in this regime. As mentioned previously, Maxfield and McLean emphasized the region near $Z=1$ and did not assume the exact BCS constants. It is not clear which procedure is best. The value of κ of Nb using $\lambda_L(0)=315$ Å and $H_c(0)=2000$ Oe is 0.85, which checks fairly well with recent values. Hopkins and Finnemore give $\kappa=0.78$, which they derive from the same $\lambda_L(0)$ of 315 Å and $dH_c(T)/dT$. Again, this small discrepancy must imply some deviation from the parabolic dependence in this regime. Finally, from the relationship that $\kappa(T\sim T_c)=0.96\lambda_L(0)/\xi_0$, we obtain that $\xi_0=356$ Å. Note that if $\lambda_L(0)$ is taken to be near 390 Å, the value quoted by Maxfield and McLean, κ would be about 1.3, using the Finnemore, Stromberg, and Swenson[20] value of $H_c\sim 2000$ Oe. This is far above the commonly accepted value of κ for Nb, and we suspect that $\lambda_L(0)$ is significantly closer to 315 rather than 390 Å.

VII. SUMMARY AND CONCLUSIONS

The tunnel-diode oscillator technique provides adequate stability for precise measurements of the field penetration into superconductors. Besides obtaining values for $\lambda_L(0)$ of 315 Å for Nb and $\lambda_L=350$ Å for Ta, a detailed discussion has been given of metallurgical problems and of the effect of normal monolayers on the temperature dependence of the measured field penetration. The solutions of the GL equations, and the data, allow estimates to be made of the $\xi(0)/b=(d\psi/dx)\,\xi(0)/\psi$. It appears that in the clean samples, $\xi(0)/b=0.02$, which corresponds to about 10 Å of normal metal. It should be emphasized that the ratio of $\xi(0)/b$ characterizes the sample surface, and it should be specified in measurements of surface properties. Actually, for low-κ materials, this effect on λ is even bigger than in the present materials, and it is possible that Al, which has a low κ, can be problematical in regard to measurements which depend sensitively on the surface.

We have found it difficult to analyze our data close to $Z=1$, where most other investigators have put their emphasis, and some disagreements have been indicated. It should be pointed out that the $\lambda_L(0)$ values for Nb obtained from the analysis near T_c, i.e., $Z>10$, check well with values of $\lambda_L(0)$ obtained from different techniques, and it appears that the analysis we have used is well justified.

ACKNOWLEDGMENTS

We are especially grateful to D. J. Sandiford and A. Joshi.

---

*This work was performed under the auspices of the U. S. Atomic Energy Commission.

†This paper is based on a thesis submitted by C. Varmazis in partial fulfillment of the Degree of Doctor of Engineering and Science at Columbia University.

[1]J. R. Hopkins and D. K. Finnemore, Phys. Rev. B 9, 108 (1974).

[2]C. Varmazis, D. J. Sandiford, and M. Strongin (unpublished).

[3]C. Boghosian, H. Meyer, and J. Rives, Phys. Rev. 146, 110 (1966).

[4]A. L. Schawlow and G. E. Devlin, Phys. Rev. 113, 120 (1959).

[5]B. Muhlschlegel, Z. Phys. 155, 313 (1959).

[6]F. London, *Superfluids* (Wiley, New York, 1950), Vol. 1.

[7]P. G. de Gennes and J. Matricon, Solid State Commun. 3, 151 (1965).

[8]L. D. Landau and E. M. Lifshitz, *Quantum Mechanics* (Pergamon, New York, 1959), Vol. 69.

[9]See, for example, M. Strongin, H. H. Farrell, H. J. Halama, O. F. Kammerer, C. Varmazis, and J. M. Dickey, Part. Accel. 3, 209 (1972).

[10]A. Joshi and M. Strongin, Scr. Metall. 8, 413 (1974).

[11]C. Varmazis, A. Joshi, T. Luhman, and M. Strongin, Appl. Phys. Lett. 24, 394 (1974).

[12]A. Joshi, C. Varmazis, M. N. Varma, and M. Strongin (unpublished).

[13]R. A. Pasternak and B. Evans, J. Electrochem. Soc. 114, 452 (1967).

[14]W. de Sorbo, Phys. Rev. 132, 107 (1963).

[15]P. B. Miller, Phys. Rev. 113, 1209 (1959).

[16]M. Strongin, H. H. Farrell, C. Varmazis, H. J. Halama, O. F. Kammerer, M. N. Varma, and J. M. Dickey, in Applied Superconductivity Conference, IEEE Publication No. 72CH0682-5-TABSC, 1972 (unpublished).

[17]E. Laurmann and D. Shoenberg, Proc. Roy. Soc. A 198, 560 (1949).

[18]B. W. Maxfield and W. L. McLean, Phys. Rev. 139,

1515 (1965).
[19]J. Auer and H. Ullmaier, Phys. Rev. B 7, 136 (1973).
[20]D. K. Finnemore, T. F. Stromberg, and C. A. Swenson, Phys. Rev. 149, 231 (1966).

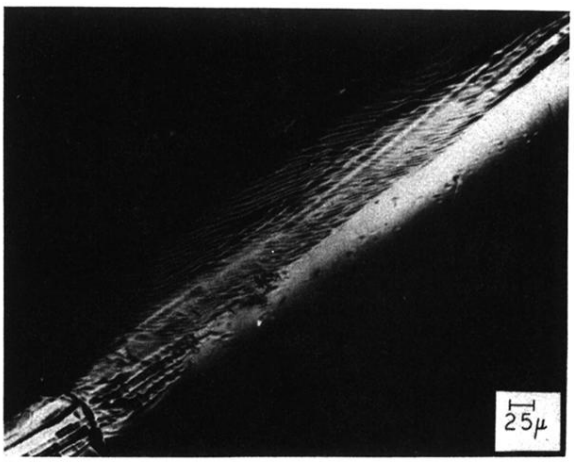

FIG. 10. Faceted surface, heated to over 1900 °C at 2×10^{-6} Torr for times of about 5 h.